MolecularMedicine

Glucagon-Like Peptide 1 Protects against Hyperglycemic-Induced Endothelial-to-Mesenchymal Transition and Improves Myocardial Dysfunction by Suppressing Poly(ADP-Ribose) Polymerase 1 Activity

Fei Yan,[1,2] Guang-hao Zhang,[1,3] Min Feng,[4] Wei Zhang,[1] Jia-ning Zhang,[5] Wen-qian Dong,[1] Cheng Zhang,[1] Yun Zhang,[1] Li Chen,[2] and Ming-Xiang Zhang[1]

[1]Key Laboratory of Cardiovascular Remodeling and Function Research, Chinese Ministry of Education and Chinese Ministry of Public Health, Qilu Hospital of Shandong University, Jinan, Shandong, China; [2]Department of Endocrinology, Qilu Hospital of Shandong University, Jinan, Shandong, China; [3]Department of Cardiology, The Second Hospital of Shandong University, Jinan, China; [4]Department of Cardiology, Affiliated Hospital of Binzhou Medical University, Binzhou, Shandong, China; and [5]School of Foreign Languages and Literature, Shandong University, Shandong, China

Under high glucose conditions, endothelial cells respond by acquiring fibroblast characteristics, that is, endothelial-to-mesenchymal transition (EndMT), contributing to diabetic cardiac fibrosis. Glucagon-like peptide-1 (GLP-1) has cardioprotective properties independent of its glucose-lowering effect. However, the potential mechanism has not been fully clarified. Here we investigated whether GLP-1 inhibits myocardial EndMT in diabetic mice and whether this is mediated by suppressing poly(ADP-ribose) polymerase 1 (PARP-1). Streptozotocin diabetic C57BL/6 mice were treated with or without GLP-1 analog (24 nmol/kg daily) for 24 wks. Transthoracic echocardiography was performed to assess cardiac function. Human aortic endothelial cells (HAECs) were cultured in normal glucose (NG) (5.5 mmol/L) or high glucose (HG) (30 mmol/L) medium with or without GLP-1analog. Immunofluorescent staining and Western blot were performed to evaluate EndMT and PARP-1 activity. Diabetes mellitus attenuated cardiac function and increased cardiac fibrosis. Treatment with the GLP-1 analog improved diabetes mellitus–related cardiac dysfunction and cardiac fibrosis. Immunofluorescence staining revealed that hyperglycemia markedly increased the percentage of von Willebrand factor (vWF)$^+$/alpha smooth muscle actin (α-SMA)$^+$ cells in total α-SMA$^+$ cells in diabetic hearts compared with controls, which was attenuated by GLP-1 analog treatment. In cultured HAECs, immunofluorescent staining and Western blot also showed that both GLP-1 analog and PARP-1 gene silencing could inhibit the HG-induced EndMT. In addition, GLP-1 analog could attenuate PARP-1 activation by decreasing the level of reactive oxygen species (ROS).Therefore, GLP-1 treatment could protect against the hyperglycemia-induced EndMT and myocardial dysfunction. This effect is mediated, at least partially, by suppressing PARP-1 activation.

Online address: http://www.molmed.org
doi: 10.2119/molmed.2014.00259

INTRODUCTION

Longstanding diabetes leads to pathogenesis of fibrotic disorders, such as diabetic cardiac fibrosis and renal fibrosis. The resultant fibrosis disrupts the normal architecture of the affected organs, ultimately leading to their dysfunction and failure (1–3). Fibroblasts are major contributors to extracellular matrix accumulation in tissue fibrosis. There is increasing evidence to show that a significant fraction of these interstitial fibroblasts is derived from the endothelium, a process called endothelial-to-mesenchymal transition (EndMT) (4–6). Recent studies suggest that the EndMT could contribute to the progression of diabetic cardiac fibrosis and renal fibrosis. Widyantoro *et al.* (7) showed that 15–20% of fibroblasts coexpressed both the endothelial marker CD31 and the fibroblast marker fibroblast-specific protein 1 (FSP1) in the hearts of diabetic WT mice. Zeisberg *et al.* (5) found that 30–50% of fibroblasts in the kidneys of diabetic mice coexpressed the endothelial marker CD31 along with FSP1-specific and alpha smooth muscle actin (α-SMA)-specific markers of fibroblasts and myofibroblasts. The current studies also indicated that blockade of EndMT

Address correspondence to *Ming-Xiang Zhang, Shandong University Qilu Hospital, Jinan, No. 107, Wen Hua Xi Road, Jinan, Shandong, 250012, China. Phone: 86-531-8216-9255; Fax: 86-531-86169356; E-mail: zhangmingxiang@sdu.edu.cn.*
Submitted December 22, 2015; Accepted for publication February 10, 2015; Published Online (www.molmed.org) February 10, 2015.

could prevent the progression of organ fibrosis (7–9).

Poly(ADP-ribose) polymerase 1 (PARP-1) is an abundant nuclear enzyme that can be activated by oxidative DNA damage, mainly reactive oxygen species (ROS) (10). On binding to damaged DNA, PARP-1 cleaves nicotine amide adenine dinucleotide (NAD^+) to produce nicotin-amide and ADP-ribose (11). When DNA damage is mild, PARP-1 participates in the DNA repair process. However, excessive activation of PARP-1 by stimuli, such as hyperglycemia, leads to intracellular depletion of NAD^+ and ATP, thus resulting in cellular energy crisis, irreversible cytotoxicity and cell death (12,13). PARP-1 activation also facilitates diverse inflammatory responses by promoting inflammation-relevant gene expression, including interleukin (IL)-1β, tumor necrosis factor (TNF)-α and endothelin-1 (14–16). These all play a significant role in fibrotic disorders. Recently, Rieder *et al.* showed that the combination of transforming growth factor (TGF)-1, IL-1 and TNF-α could induce EndMT in human intestinal microvascular endothelial cells (17). Widyantoro *et al.* (7) also demonstrated that endothelin-1 gene silencing could inhibit hyperglycemia-induced EndMT in cultured endothelial cells. However, it is still unclear whether PARP-1 inhibition could suppress hyperglycemia-induced EndMT.

Glucagon-like peptide-1 (GLP-1) is an incretin hormone produced by intestinal L cells in response to food intake. Emerging evidence has shown the antiinflammatory effects of GLP-1 on the cardiovascular system. In fact, it has been reported that GLP-1 analogs could ameliorate cardiac steatosis in diet-induced obesity (DIO) mice or type 2 diabetes mice (18,19). However, in those studies, after systemic administration of GLP-1 analogs, the mice also showed an improvement in blood glucose and insulin sensitivity, both of which play significant roles in cardiac fibrosis (20, 21). Thus, the molecular mechanisms by which GLP-1 caused the antifibrotic effects are still controversial. We recently demonstrated that GLP-1 could protect microvascular endothelial cells by inactivating the PARP-1–inducible nitric oxide (NO) synthase–NO pathway (22). On the basis of these findings, we wondered whether GLP-1 could inhibit myocardial EndMT in diabetic mice and whether this was mediated by inactivating PARP-1. Accordingly, we designed this study to determine the protective effects of GLP-1 on hyperglycemia-induced EndMT and to characterize the underlying molecular mechanism.

MATERIALS AND METHODS

Reagents and Antibodies

Human aortic endothelial cell (HAEC) medium (endothelial cell medium [ECM]) and fetal bovine serum (FBS) were Gibco products (Thermo Fisher Scientific Inc., Waltham, MA, USA); exenatide acetate (GLP-1 analog) was from Huayi BIO-Lab (Shanghai, China); *N*-acetyl-L-cysteine (NAC) and diacetate (DCFH-DA) were from Sigma-Aldrich (St. Louis, MO, USA); Lipofectamine 2000 was from Life Technologies (Thermo Fisher Scientific); small interfering RNA duplexes against PARP-1 (siPARP-1), small interfering RNA duplexes against Snail (siSnail) and the negative control (si-NC) were from GenePharma (Shanghai, China). The primary antibody β-actin, VE-cadherin and poly(ADP-ribose) (PAR) were from BD Biosciences (San Jose, CA, USA). Matrix metalloproteinase (MMP)-2, MMP-9, and collagen I and III were from Santa Cruz Biotechnology (Santa Cruz, CA, USA). Secondary antibodies were Invitrogen products (Thermo Fisher Scientific).

Cell Culture and Treatment

HAECs (ATCC, Manassas, VA, USA) were cultured in ECM supplemented with 5% FBS, 100 U/mL penicillin and 100 μg/mL streptomycin at 37°C. The culture medium was changed to a serum-free solution for 12 h, and then cells were treated with 5 mmol/L D-glucose (normal glucose [NG]) or 30 mmol/L D-glucose (high glucose [HG]) for 3 d. The medium was changed every 24 h. siPARP-1, siSnail and si-NC duplexes were transfected into HAECs by using Lipofectamine 2000. Then cells were exposed to HG with or without 50 nmol/L GLP-1, or 10 nmol/L NAC (an inhibitor of ROS) after a 24-h transfection for 72 h. We used cells at no more than passage 4.

Western Blot Analysis

Equal amounts of protein were separated on 10% SDS-PAGE and electrotransferred onto nitro-cellulose membranes (Amersham Biosciences [GE Healthcare Bio-Sciences, Pittsburgh, PA, USA]), which were blocked with 5% nonfat milk for 2 h at room temperature, washed three times for 10 min, and incubated overnight at 4°C with primary antibodies against PARP-1, α-SMA, Snail, β-actin, VE-cadherin, PAR, MMP-2, MMP-9 or collagen I or III and then horseradish peroxidase–conjugated secondary antibody for 1 h at room temperature. Blots were visualized by chemiluminescence (Millipore, Billerica, MA, USA).

ROS Production Assay

HAECs were washed twice with phosphate-buffered saline (PBS) and then incubated with 2,7-dichlorofluoresceindiacetate (H2DCF-DA) for 30 min at 37°C. ROS level was determined by the oxidative conversion of H2DCF-DA to fluorescent dichlorofluorescein on reaction with ROS in cells. HAECs were incubated with dihydroethidium for 30 min at room temperature. After a washing with PBS, fluorescent signals (ROS, 488 nm) were acquired by using a Zeiss LSM 710 confocal microscope. Three independent experiments were performed.

Gelatin Zymography

The relative amount of MMP-2 and MMP-9 protein in HAECs was measured by gelatin zymography. The culture supernatant was harvested and mixed with a gel sample buffer (0.5 mol/L Tris-HCl, glycerol, 10% sodium dodecyl sulfate [SDS], β-mercaptoethanol and 0.5% bro-

mophenol blue). An amount of 10 μg protein was separated by SDS–polyacrylamide gel electrophoresis with 0.1% gelatin (Sigma-Aldrich). After electrophoresis, gels were washed with 50 mmol/L Tris buffer containing 2.5% Triton X-100. Gels were incubated for an additional 24 h in incubation fluid (50 mmol/L Tris buffer, 10 mmol/L $CaCl_2$ and 200 mmol/L NaCl) and then stained with 0.5% Coomassie blue containing 30% methanol and 10% glacial acetic acid and destained in 45% methanol/10% acetic acid/H_2O. White bands on a blue background indicated zones of digestion corresponding to the presence of different MMPs. Gels were scanned, and analysis of bands involved use of ImageJ (NIH, Bethesda, MD, USA).

Animal Model

C57BL/6J male mice (n = 80, 8 wks old, 25–30 g) were purchased from The Jackson Laboratory (Bar Harbor, ME, USA), housed at a constant temperature (24°C) and given a normal diet with free access to water. Nondiabetic mice were used as controls (n = 26). Diabetes mellitus (DM) was induced by multiple low-dose (50 mg/kg) intraperitoneal injection of streptozotocin (STZ) as described (23). Blood samples for glucose measurements were taken from the tail vein ~48 h after STZ injection. All mice with nonfasting glucose levels of 13.8 mmol/L were considered diabetic and received no insulin treatment. One month after diabetes onset, diabetic mice were randomly divided into two groups for treatment (n = 26 each): daily saline (DM alone) and GLP-1 analog (24 nmol/kg daily; DM + GLP-1) (18). After 24 wks of diabetes, mice were sacrificed. Plasma samples were collected by heart puncture by using a heparinized syringe after mice were anesthetized. Blood glucose concentrations were measured by using a Breese 2 glucose meter (Bayer HealthCare, Leverkusen, Germany). Plasma insulin levels were measured with a Linco insulin ELISA (enzyme-linked immunosorbent assay) kit. All experiments were performed in compliance with the *Guide for the Care and Use of Laboratory Animals* (24) and in compliance with Shandong University.

Table 1. Basic parameters of mice with DM and GLP-1 analog treatment.

Parameters	Controls (n = 9)	DM (n = 9)	DM+GLP-1 (n =9)
Fasting blood glucose (mmol/L)	56 ± 1.8	16.1 ± 4.5[a]	15.5 ± 3.5[b]
Nonfasting blood glucose (mmol/L)	8.3 ± 2.3	25.9 ± 7.7[a]	24.3 ± 4.6[b]
Systolic blood pressure (mmHg)	112 ± 5.1	130 ± 9.2[a]	125 ± 7.4[b]
Diastolic blood pressure (mmHg)	87 ± 5.2	102 ± 4.6[a]	99 ± 72[b]
Body weight (g)	28.7 ± 3.4	21.8 ± 5.1[a]	22.6 ± 4.5[b]
Fasting insulin (ng/mL)	0.82 ± 0.19	0.15 ± 0.07[a]	0.18 ± 0.05[b]
Nonfasting insulin (ng/mL)	2.11 ± 0.55	0.21 ± 0.15[a]	0.25 ± 0.12[b]

Data are means ± SD.
[a]$p < 0.05$ compared with controls.
[b]$p < 0.05$ compared with DM alone.

Cardiac Function Measurement

Transthoracic echocardiography was performed 24 wks after STZ injection. Mice were anesthetized with isoflurane mixed with O_2 at a flow rate of 5 psi. Cardiac diameter and function were measured by use of the Vevo770 imaging system equipped with a high-frequency ultrasound probe. M-mode images of the parasternal long- and short-axis views of the left ventricle were obtained. Left ventricular ejection fraction and fractional shortening were calculated by using Vevo 770 software.

Immunocytochemistry and Immunohistochemistry

Frozen heart tissues were transversely cut at 5-μm thickness and fixed in 100% acetone at –20°C for 10 min. HAECs were fixed in 4% paraformaldehyde for 20 min. Then tissue sections or cells were permeabilized in 0.03% Triton X-100 for 15 min. After being blocked in 5% bovine serum albumin for 30 min at room temperature, cells were incubated with primary antibodies for PAR, Snail, α-SMA or VE-cadherin at 4°C overnight and then with a fluorescence dye–conjugated secondary antibody. Nuclei were visualized with 4′6-diamidino-2-phenylindole·2HCl (DAPI) (Santa Cruz Biotechnology).

Paraformaldehyde (4%) fixed hearts were bisected transversely at the mid-ventricular level, embedded in paraffin and cut into 5-μm-thick sections and then stained with Masson staining. Dark green–stained collagen fibers were quantified as a measure of fibrosis and examined by light microscopy in a blinded manner. To normalize the perivascular collagen area around vessel with different sizes, perivascular fibrosis was calculated as the ratio of the fibrotic area surrounding the vessels to the total vessel area. The intramyocardial and perivascular collagen area were quantified digitally by using Image-Pro Plus 6.2 (Media Cybernetics Inc., Rockville, MD, USA).

Quantitation of Fibroblasts of Endothelial Cell Origin

Cells that coexpressed both the endothelial marker von Willebrand factor (vWF) and the myofibroblast marker α-SMA were counted in the hearts. Five areas were randomly selected and analyzed at 400× magnification in each of five sections from each heart. The percentage of $vWF^+/\alpha\text{-}SMA^+$ cells in total $\alpha\text{-}SMA^+$ cells and the percentage of $\alpha\text{-}SMA^+$ cells in total cells were determined.

Cell Migration Assay

Cell motility was examined by scratch assay as described (25). Cells were seeded in 12-well plates at 1.0×10^5 cells per well and incubated plates at 37°C until cells reached 100% confluence. An artificial gap was generated by scratching with use of a 200-μm pipette tip. Photographic images were taken immediately and after 12 h with a digital camera system. The software program HMIAS-2000 was used to calculate the cell migration distance (μm). Each experiment was repeated at least three times.

A

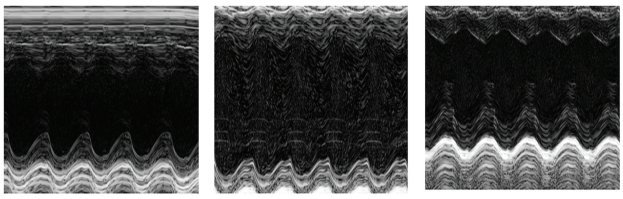

B

Parameters	Control (n = 9)	DM (n = 9)	DM + GLP-1 (n =9)
LVEDd (mm)	2.08 ± 0.11	3.1 ± 0.15#	2.7 ± 0.13*
IVS (mm)	0.67 ± 0.03	0.69 ± 0.04	0.67 ± 0.06
LVPWd (mm)	1.21 ± 0.04	1.12 ± 0.05	1.19 ± 0.03
LVEF (%)	75.2 ± 2.4	59.1 ± 1.1#	65.3 ± 3.3*
FS (%)	35.4 ± 1.8	22.4 ± 3.3#	31.3 ± 2.4*
E/A	1.5 ± 0.3	0.8± 0.2#	1.2± 0.2*

Figure 1. GLP-1 improves cardiac function in diabetic mice. n = 9 mice for each group. (A) Representative M-mode echocardiograms. (B) LVEDd, left ventricular end-diastolic dimension; IVS, interventricular septum thickness; LVPWd, left ventricular diastolic posterior wall thickness; LVEF, left ventricular ejection fraction; FS, fractional shortening, calculated; E/A, E: peak velocity at early diastole. A: peak velocity at late diastole. Data are mean ± SD; n = 9 per group. $^{\#}p < 0.05$ versus control, $^{*}p < 0.05$ versus DM.

Statistical Analysis

Data are expressed as mean ± standard deviation (SD). An independent Student *t* test was used for comparison between groups and one-way analysis of variance for comparison among multiple groups with *post hoc* Bonferroni correction. SPSS v12.0 for Windows (SPSS, Chicago, IL) was used for analysis. $p < 0.05$ was considered statistically significant.

RESULTS

Basic Characteristics of Mice

At 24 wks, the DM group had significantly higher fasting blood glucose and higher systolic and diastolic blood pressures, as well as lower body weight compared with controls ($p < 0.05$) (Table 1). GLP-1 had no effect on blood glucose, blood insulin, blood pressure or body weight.

GLP-1 Attenuates Myocardial Fibrosis and Cardiac Dysfunction in Mice with DM

Cardiac function was assessed by using transthoracic echocardiogram at 24 wks. At 24 wks, cardiac function was lower in diabetic than control mice: left ventricular ejection fraction (59.1 ± 1.1 versus 75.2 ± 2.4, $p < 0.05$), fractional shortening (35.4 ± 3.3 versus 22.4 ± 1.8, $p < 0.05$), ratio of peak early diastolic ventricular filling velocity to peak atrial filling velocity (E/A ratio, 0.8 ± 0.2 versus 1.5 ± 0.3, $p < 0.05$) and left ventricular end-diastolic dimension (3.1 ± 0.15 versus 2.08 ± 0.15, $p < 0.05$) (Figures 1A, B). Compared with DM alone, GLP-1 treatment ameliorated the altered parameter values.

Masson trichome staining of heart sections revealed increased ECM deposition in the perivascular and intramyocardial regions of the diabetic mouse myocardium compared with controls (Figures 2A–C). Diabetes was associated with a 3.25- and 3.11-fold increase in collagen deposition in the perivascular and intramyocardial regions, respectively, compared with controls (8.35 ± 1.23% versus 2.57 ± 3.17%, $p < 0.05$, and 16.2 ± 1.67% versus 5.21 ± 2.39%, $p < 0.05$) GLP-1 analog treatment significantly reduced collagen deposition compared with DM alone. In addition, diabetes increased the expression of fibrotic markers collagen I and III compared with controls, and GLP-1 analog treatment significantly reduced the levels compared with DM alone ($p < 0.05$; Figures 2D, E).

GLP-1 Inhibits HG-Induced EndMT *In Vitro* and *In Vivo*

EndMT has been shown in previous studies to contribute to the progression of diabetic cardiac fibrosis. We therefore proceeded to determine whether the antifibrotic effect of GLP-1 is associated with EndMT *in vitro* and *in vivo*. For the *in vivo* study, we chose vWF (an endothelial cell marker expressed in plasma) and α-SMA (a myofibroblast marker expressed in plasma) to illustrate the effects of GLP-1 on HG-induced EndMT. Immunofluorescence staining of mouse hearts after 24 wks of GLP-1 treatment revealed that DM markedly increased the proportion of cells expressing α-SMA by 4.23-fold compared with controls (16.53 ± 4.56 versus 3.91 ± 1.23; $p < 0.05$), which was reduced with GLP-1 treatment (11.35 ± 2.78; $p < 0.05$). The proportion of cells expressing both vWF and α-SMA in the cardiac tissue was lower after GLP-1 treatment, compared with DM alone (21.33 ± 3.75 versus 12.61 ± 2.23; $p < 0.05$) (Figures 3A–C). *In vitro*, HAECs were treated with or without GLP-1 for 72 h under HG conditions. Fluorescence microscopy revealed that while control HAECs had the typical rounded or cobblestone shape, HG-treated HAECs acquired a spindle-shaped morphology. This change in morphology was inhibited by GLP-1 treatment (Figure 3D). Immunofluorescence demonstrated that HG-treated cells acquired mesenchymal marker α-SMA staining (a myofibroblast marker) and lost endothelial marker VE-cadherin (also the endothelial cell-to-cell contact regulator) staining compared with controls (Figure 3E).

GLP-1 Decreased HG-Induced PARP-1 Expression and Activity by Suppressing ROS Production in HAECs

ROS plays a major role in diabetic cardiovascular disease and damaged DNA, which leads to PARP-1 activation. We therefore conducted an experiment to

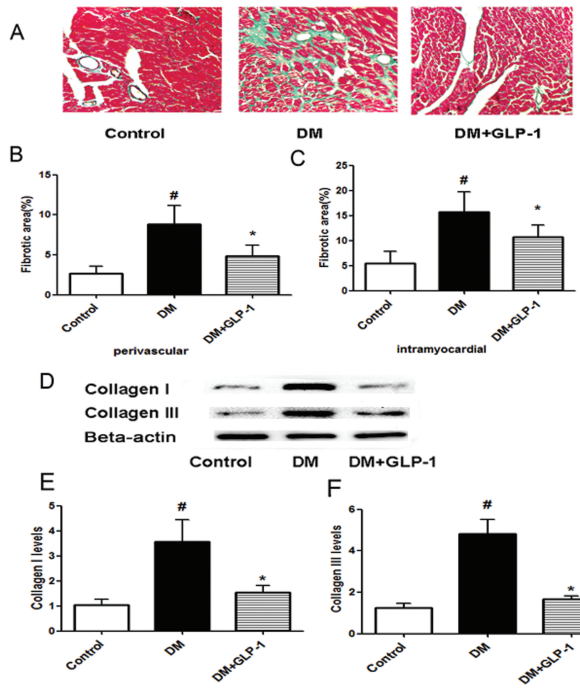

Figure 2. GLP-1 suppresses cardiac fibrosis in diabetic mice. n = 6–7 mice for each group. (A) Masson trichrome staining of mouse hearts. (B, C) Quantification of fibrotic areas in the perivascular and interstitial region. Data are mean ± SD. $^{\#}p < 0.05$ versus control, $^{*}p < 0.05$ versus DM. (D–F) Western blot analysis of collagen I and III expression. Data are mean ± SD. $^{\#}p < 0.05$ versus control, $^{*}p < 0.05$ versus DM.

determine whether GLP-1 attenuated HG-induced PARP-1 expression and activity by suppressing ROS production. ROS production increased more than threefold under HG conditions ($p < 0.05$) but decreased significantly with both GLP-1 and NAC (ROS inhibitor, as a positive control) treatment ($p < 0.05$) in HAECs (Figures 4A, B). The expression and activity of PARP-1 were significantly increased by about 1.8- and 2.73-fold with HG compared with controls ($p < 0.05$) but were decreased with GLP-1 or NAC treatment ($p < 0.05$) (Figures 4C, D).

GLP-1 Inhibited HG-Induced EndMT by Suppressing PARP-1 Activation

To further determine the molecular mechanisms for the inhibitory effect of GLP-1 on EndMT, HAECs were transfected with PARP-1 siRNA or Snail (the key factor that regulates the EndMT, which is used for positive control) siRNA or treated with GLP-1. HAECs with NG treatment expressed the endothelial

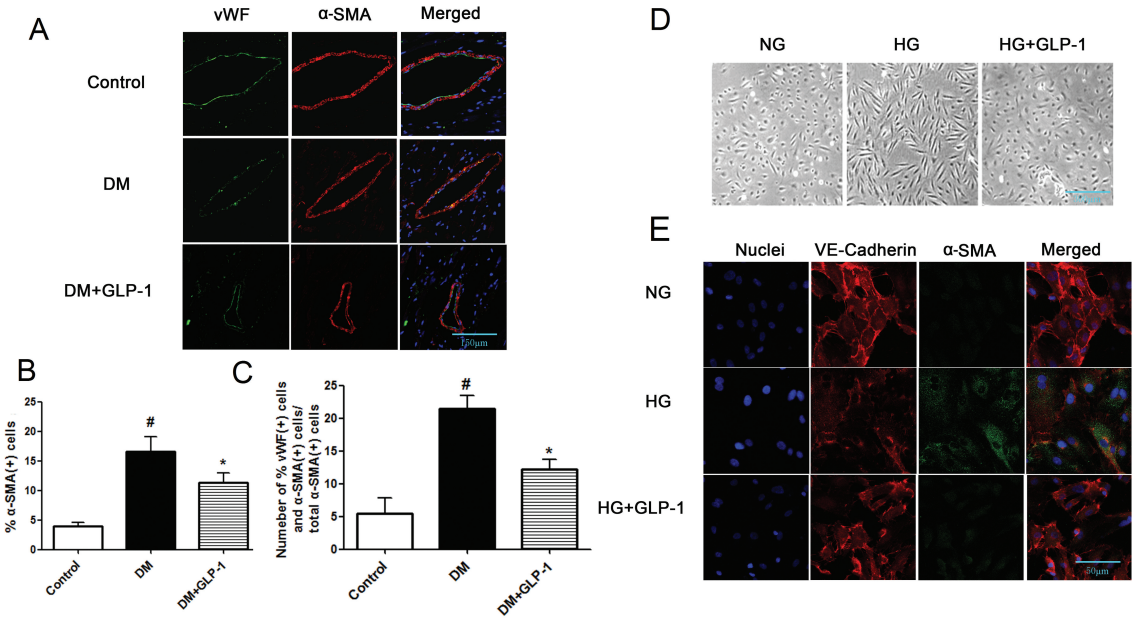

Figure 3. GLP-1 inhibited HG-induced EndMT *in vitro* and *in vivo*. (A) Confocal microscopy of vWF (green), α-SMA (red), DAPI (blue) in mouse diabetic hearts. Colocalization of vWF and α-SMA expression in heart tissues in yellow. (B) Quantification of α-SMA staining cells in diabetic hearts. (C) vWF and α-SMA staining quantification to total α-SMA staining in diabetic hearts. (D) Morphological changes in HAECs were observed by microscopy (10×). (E) Immunofluorescence staining with antibodies to VE-cadherin (red) and α-SMA (green). Nuclei were counterstained with DAPI (blue nuclei). Data are mean ± SD; n = 6–7 per group. $^{\#}p < 0.05$ versus control; $^{*}p < 0.05$ versus DM.

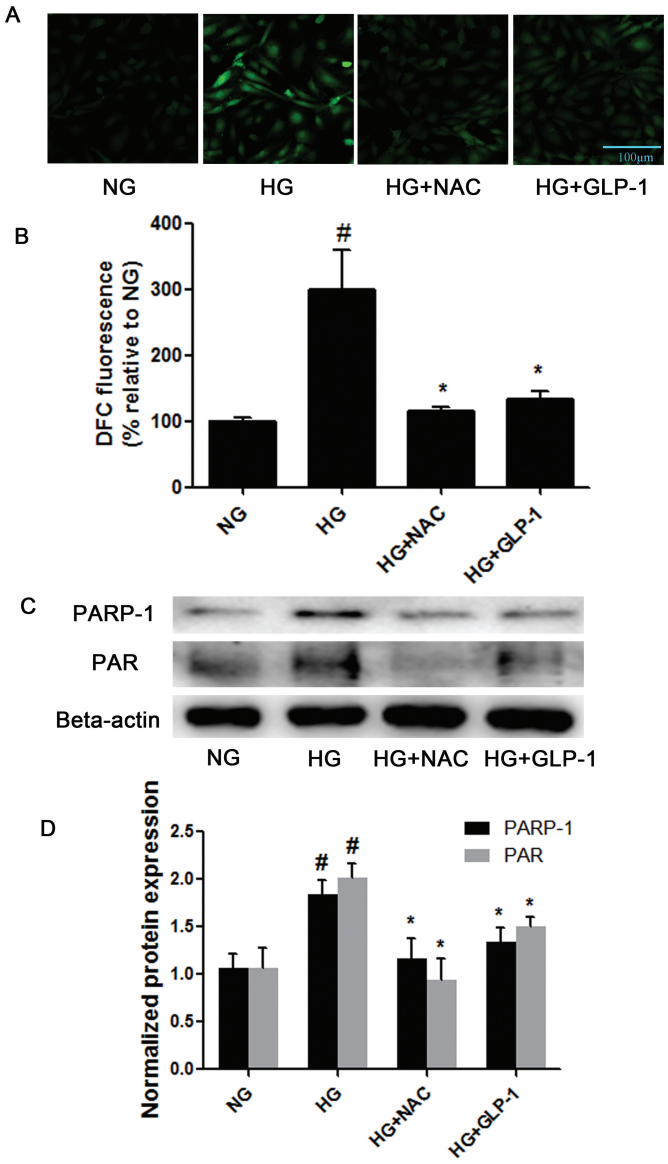

Figure 4. GLP-1 inhibited HG-induced PARP-1 expression and activity by reducing ROS production in HAECs. Immunofluorescent staining of intracellular ROS production (A) and quantification with and without NAC and GLP-1 (B) are shown. (C, D) Western blot analysis of PARP-1 and PAR protein expression. Results are from three repeated experiments. Data are means ± SD. $^{\#}p < 0.05$ versus NG, $^{*}p < 0.05$ versus HG.

markers VE-cadherin, whereas HAECs with HG treatment showed lower VE-cadherin and higher α-SMA expression. Treatment with siPARP-1, siSnail or GLP-1 markedly inhibited HG-induced α-SMA expression (Figures 5A, B). These results therefore suggest that GLP-1 may mitigate HG-induced EndMT by suppressing PARP-1 activation.

GLP-1 Inhibits HG-Induced EndMT by Suppressing PARP-1–Snail Interaction

Because Snail is also considered an EndMT initiating factor (26), we examined the effects of GLP-1 on Snail expression in HAECs with or without HG treatment. Incubation of HAECs with HG significantly upregulated PARP-1 expression and activity, increased Snail expression (Figures 6A–D) and markedly increased PARP-1–Snail interaction in the nuclei (Figure 6E). Treatment with GLP-1 significantly reduced PARP-1 and Snail expression and interaction (Figures 6A–D). GLP-1 and siPARP-1 treatment markedly reduced PARP-1 and PAR protein level compared with HG treatment. However, Snail silencing had no effect on PARP-1 or PAR protein level compared with HG treatment ($p < 0.05$) (Figures 6A–D). Therefore, our results suggested that GLP-1 could inhibit HG-induced EndMT by suppressing PARP-1–Snail interaction.

GLP-1 Reduced HG-Induced Collagen I and III and MMP-2 and MMP-9 Expression by Inhibiting EndMT

Cells undergoing EndMT play a key role in fibrosis by increasing the production of collagen I and III, MMP-2 and MMP-9. To test the function of HAECs undergoing EndMT, we measured the protein expression of collagen I and III. Incubating HAECs in HG greatly increased the protein expression of collagen I and III compared with NG. Treatment with GLP-1 or siPARP-1 or siSnail markedly decreased HG-induced collagen I and III expression ($p < 0.05$) (Figures 7A, B). Moreover, gelatin zymography revealed that HG treatment significantly increased the activity of MMP-2 and MMP-9 compared with NG. GLP-1, siPARP-1 or siSnail treatment markedly reduced HG-induced MMP-2 and MMP-9 activity ($p < 0.05$) (Figures 7C, D).

GLP-1 Inhibits HG-Induced Cell Migration by Suppressing EndMT

Some studies suggest that loss of VE-cadherin and increase in the activity of enzymes (MMP-2 and MMP-9) involved in ECM degradation during EndMT increases migration capability of endothelial cells (7,27). This result led us to examine the cell migration capability in our *in vitro* study. We performed a scratch assay and found that HG in-

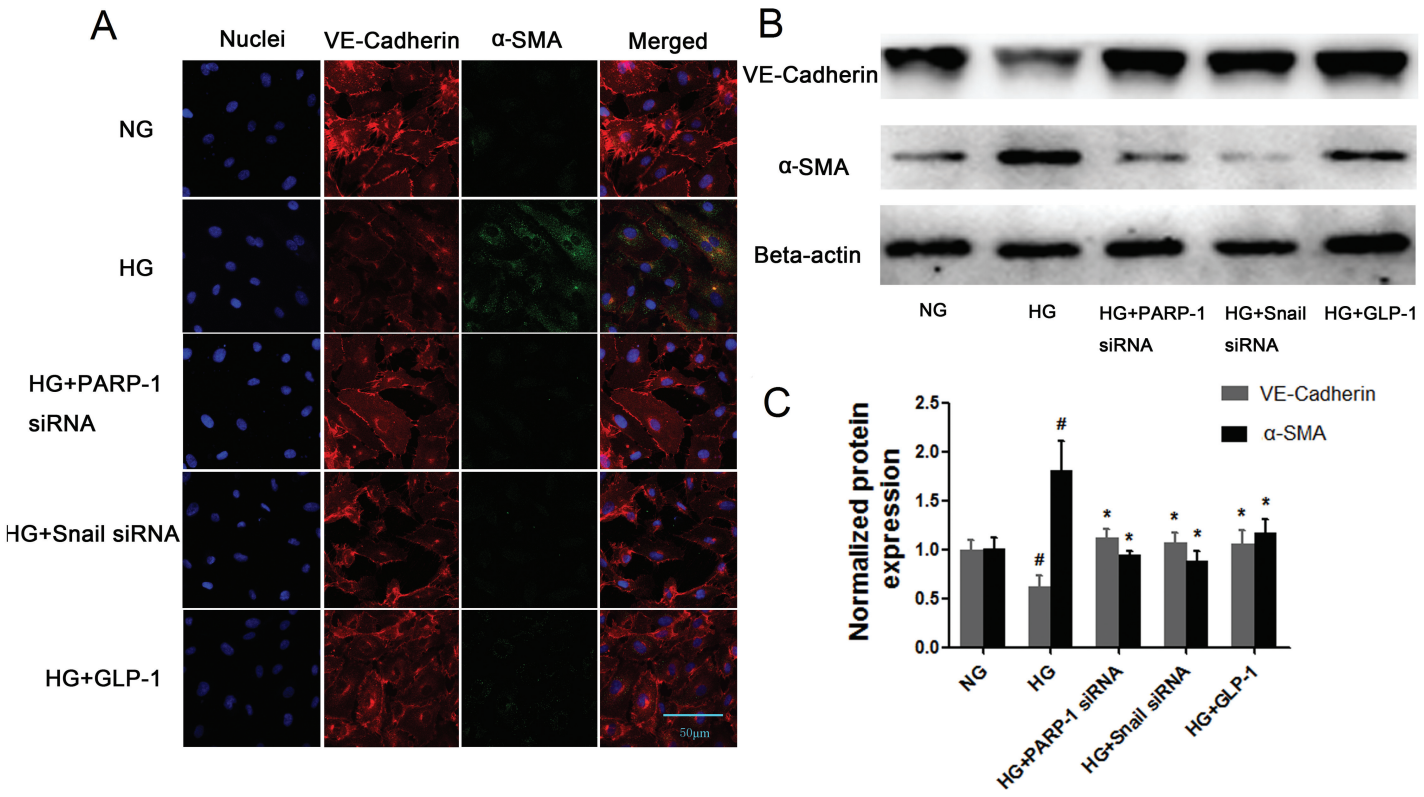

Figure 5. (A) GLP-1 inhibited HG-induced EndMT by suppressing PARP-1 activation. Immunofluorescence staining of VE-cadherin (red) and α-SMA (green) is shown. Nuclei were counterstained with DAPI (blue). (B, C) VE-cadherin and α-SMA expression were determined by Western blot analysis. Results are from three repeated experiments.

creased cell migration compared with NG. After 12 h of incubation with HG, the gap distance was significantly reduced by over 80% compared with baseline control (Figures 8A–C). Both GLP-1 and PARP-1 gene silencing significantly prevented the decrease in gap distances at 12 and 24 h ($p < 0.01$). Furthermore, immunofluorescence indicated that cells with faster migration capability were the transitioned endothelial cells (Figure 8C).

DISCUSSION

Glucagon-like peptide-1 (GLP-1) has cardioprotective properties independent of its glucose-lowering effect. However, the underlying mechanisms have not been fully elucidated. Recent studies showed that EndMT plays a significant role in diabetes mellitus–induced cardiac dysfunction. Here we report that GLP-1 treatment could protect against hyperglycemia-induced EndMT and myocardial dysfunction. This effect is mediated, at least partially, by suppressing PARP-1 activation.

GLP-1, an intestinally derived hormone, reduces blood glucose levels by increasing the secretion of insulin (28). We and others have previously observed that GLP-1 can exert significant antiinflammatory effects through GLP-1–specific receptors that are found in the heart, vascular smooth cells and endothelial cells (29–31). In fact, it has been reported that GLP-1 analogs can ameliorate cardiac steatosis in DIO mice or type 2 diabetes mice (18,19). However, in those studies, after systemic administration of GLP-1 analog, the mice also showed an improvement in blood glucose and insulin sensitivity, both of which play significant roles in cardiac fibrosis (20,21). Thus, the molecular mechanisms by which GLP-1 caused the antifibrotic effects are still controversial. In this study, we hypothesize that GLP-1 analog treatment has a protective effect against cardiac fibrosis via an insulin- and glucose-independent mechanism in a STZ-induced type 1 diabetes model. Similar to previous studies (7,9), the DM group showed significantly increased intramyocardial and perivascular fibrosis and impaired cardiac diastolic function compared with controls. Chronic GLP-1 analog administration markedly reduced myocardial fibrosis and cardiac dysfunction in STZ-induced diabetic mice.

To elucidate the mechanism through which GLP-1 reduces myocardial fibrosis and improves cardiac function, we focused on myofibroblasts in the fibrotic area. Increasing evidence shows that a significant fraction of these myofibroblasts are derived from the endothelium via a process called endothelial-to-

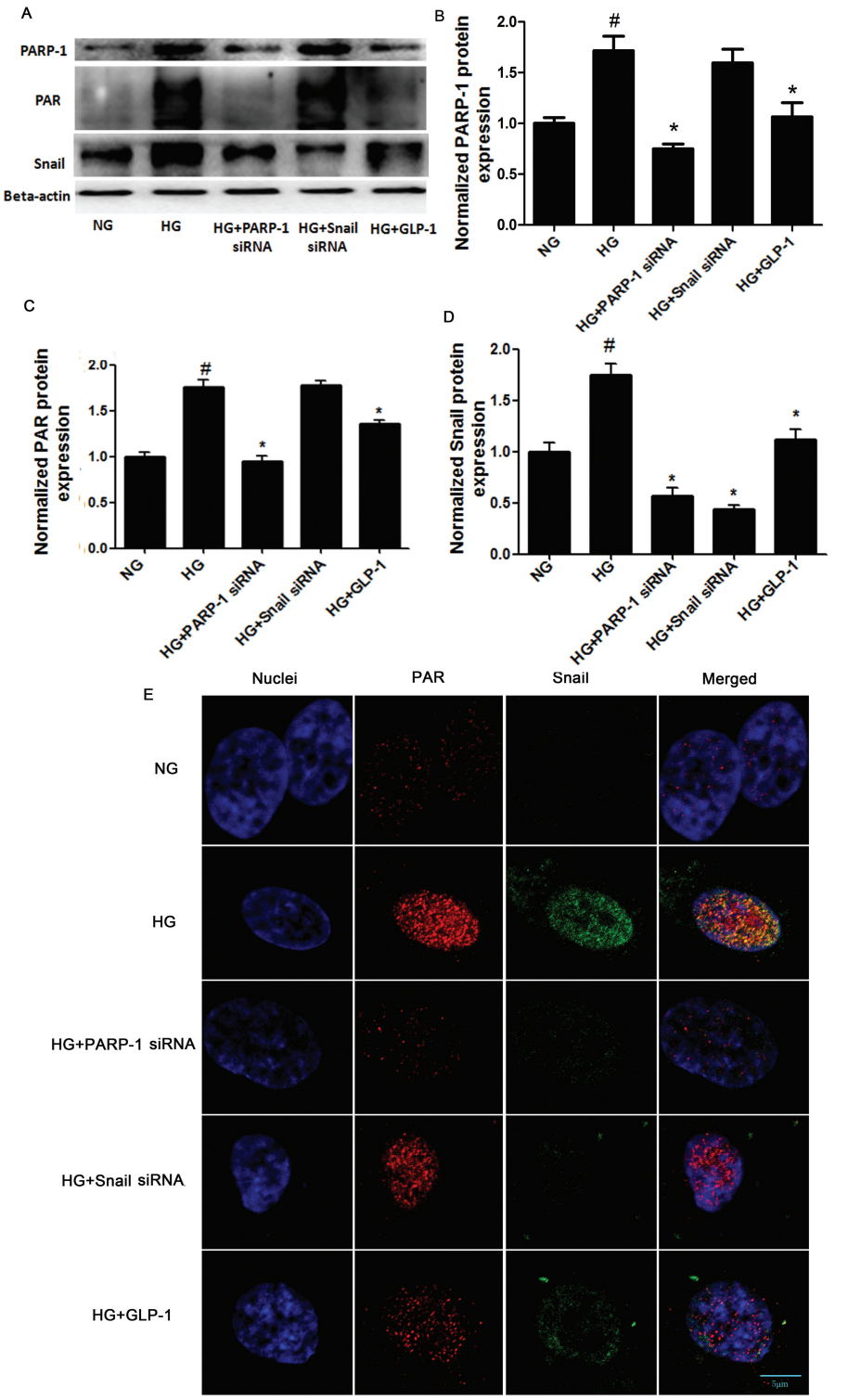

Figure 6. GLP-1 reduced HG-induced Snail expression by suppressing PARP-1 activation in HAECs. (A–D) PARP-1, PAR and Snail expression were determined by Western blot analysis. (E) Nuclear colocalization of PAR and Snail was analyzed by double immunofluorescence. The red staining represents PAR and the green staining Snail. Results are from three repeated experiments. Data are mean ± SD. $^{\#}p < 0.05$ versus NG, $^{*}p < 0.05$ versus HG.

mesenchymal transition (EndMT) (32,33). Fibroblasts derived from the endothelial lineages can also function as resident tissue fibroblasts that produce massive ECM proteins and ECM degrading enzymes in fibrotic disorders. Chronic hyperglycemia is an important initiator of EndMT. In this study, we observed that in the cardiac tissue of diabetic mice, the proportion of α-SMA^{+} cells that coexpress vWF was much greater than that in nondiabetic mice. In addition, GLP-1 treatment significantly reduced the percentage of vWF^{+}/α-SMA^{+} cells. The reason that we chose vWF instead of VE-cadherin *in vivo* is because vWF is an endothelial cell marker expressed in plasma, which could reflect the proportion of transitioned cells more clearly *in vivo* compared with the markers expressed on the membrane under a confocal microscope. Several previous studies also used this marker to detect EndMT *in vivo* (8,17), which could clearly support our results. To further confirm our *in vivo* observations, we conducted *in vitro* experiments with HAECs incubated with HG. Similar to our *in vivo* study, incubation of HAECs with HG resulted in decreased levels of the endothelial marker VE-cadherin (also endothelial cell-to-cell regulator) and increased expression of the myofibroblast (the functional fibroblast) marker α-SMA. These effects were markedly reversed with GLP-1 analog treatment.

PARP-1, the DNA repair–associated nuclear enzyme, is involved in the development of various diabetic complications, including diabetic cardiomyopathy, diabetic nephropathy, diabetic cystopathy and diabetic retinopathy (23,34,35). Hyperglycemia can lead to overproduction of mitochondrial ROS, which then activates PARP-1 (13). PARP-1 activation can induce inflammation-relevant factors such as IL-1, endothelin-1, TGF-1 and Smad3 (14,15), which are closely related to EndMT. In the present study, we found that HG not only increased PARP-1 activation and Snail (the key regulator that mediates

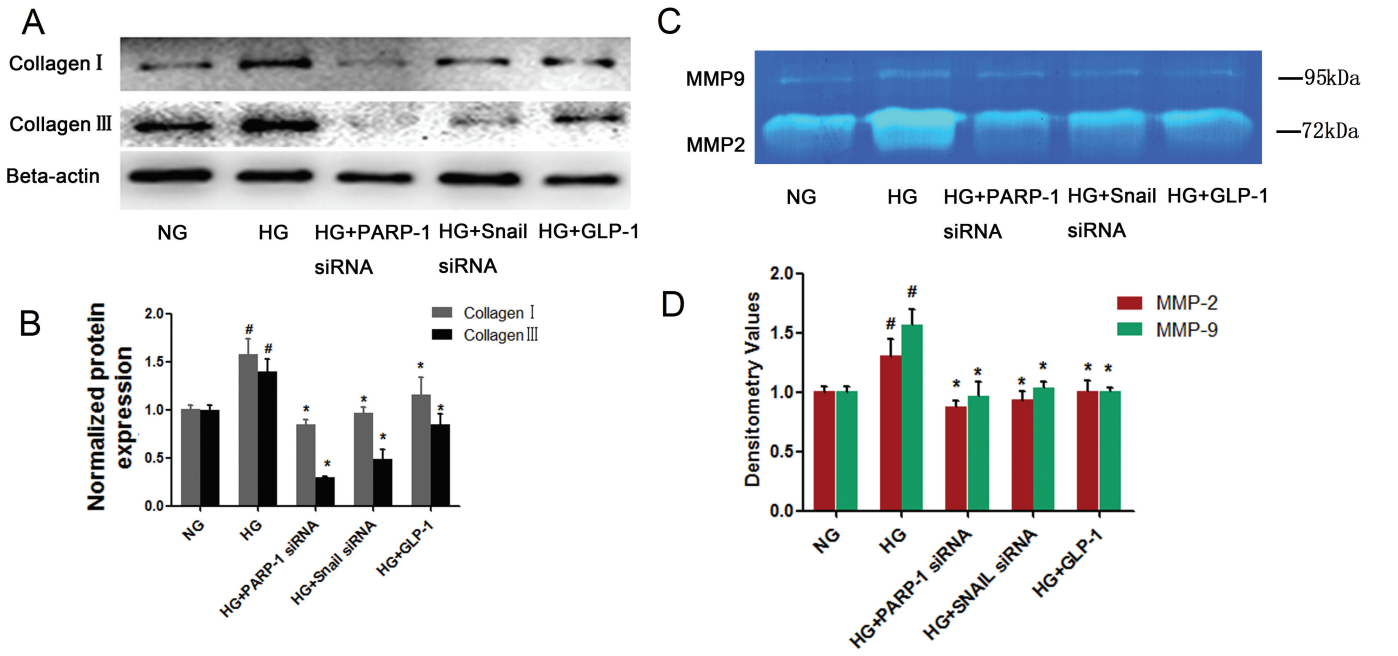

Figure 7. GLP-1 reduced HG-induced collagen I, collagen III, MMP-2 and MMP-9 expression in HAECs with siPARP-1 or GLP-1. (A, B) Western blot analysis of collagen I and III expression. Data are mean ± SD. $^{\#}p < 0.05$ versus NG, $^{*}p < 0.05$ versus HG. (C, D) Gelatin zymography analysis of MMP-2 and MMP-9 activity. Results are from three repeated experiments. Data are mean ± SD. $^{\#}p < 0.05$ versus NG, $^{*}p < 0.05$ versus HG.

EndMT) expression, it also facilitated the colocalization of PAR and Snail in the nuclei. Furthermore, *PARP-1* gene silencing reduced Snail expression and inhibited hyperglycemia-induced EndMT in HAECs. According to a recent study, PARP-1, but not PARP-2, increased Snail protein stability by poly(ADP-ribosyl)ation of Snail in human melanoma cells (36). Thus, our results suggest that PARP-1 may act as an upstream regulator in hyperglycemia-induced EndMT.

On the basis of our previous study, GLP-1 can effectively protect MS1 cells against oxidized low-density lipoprotein–induced apoptosis by inactivating PARP-1 (22). There is also growing evidence to support that GLP-1 can reduce hyperglycemia-induced ROS accumulation via protein kinase A–mediated inhibition of NAD(P)H oxidases (37–39) and that ROS is a significant stimulus for PARP-1 activation (13). These findings led us to further investigate the potential mechanisms of GLP-1 in HG-induced PARP-1 activation and EndMT. In this study, we found that GLP-1 attenuated PARP-1 activity and Snail expression in HAECs under HG conditions. In addition, immunofluorescent staining showed that GLP-1 inhibited hyperglycemia-induced PAR and Snail colocalization in the nuclei of HAECs. This inhibitory effect of GLP-1 on PARP-1 may be secondary to reduced ROS production.

Although endothelial cells acquired a myofibroblast-phenotype under HG conditions, we were not sure whether these transitioned cells could function as fibroblasts. Therefore, we performed Western blot and gelatin zymography to test the function of these transitioned cells *in vitro*. As predicted, endothelial cells incubated under HG conditions could produce massive amounts of ECM proteins (collagen I and III) and ECM degradative enzymes (MMP2 and MMP9). After Snail, the key regulator of EndMT, was knocked out, all these effects were abolished. These results confirm our hypothesis that transitioned cells not only acquire the myofibroblast-phenotype, but also the myofibroblast-function. Similar results were obtained when cells were treated with GLP-1 or PARP-1 siRNA.

EndMT was preceded by loss of endothelial cell-to-cell contact, as shown by decreased VE-cadherin expression and increased ECM degrading enzymes such as MMP-2 and MMP-9 (7,27). The disaggregated endothelial cells then start to alter their structure, migrate to surrounding sites, decrease expression of endothelial marker and acquire mesenchymal characteristics. Therefore, we performed scratching assay to evaluate the cell migration ability. In concordance with previous data (7), we observed that hyperglycemia promotes endothelial cell migration, with the transitioned cells having the highest migration capability. Our results also indicated that GLP-1 treatment or PARP-1 gene silencing significantly prevented cell migration. This effect is probably associated with increased VE-cadherin and decreased MMP-2 and MMP-9 activity.

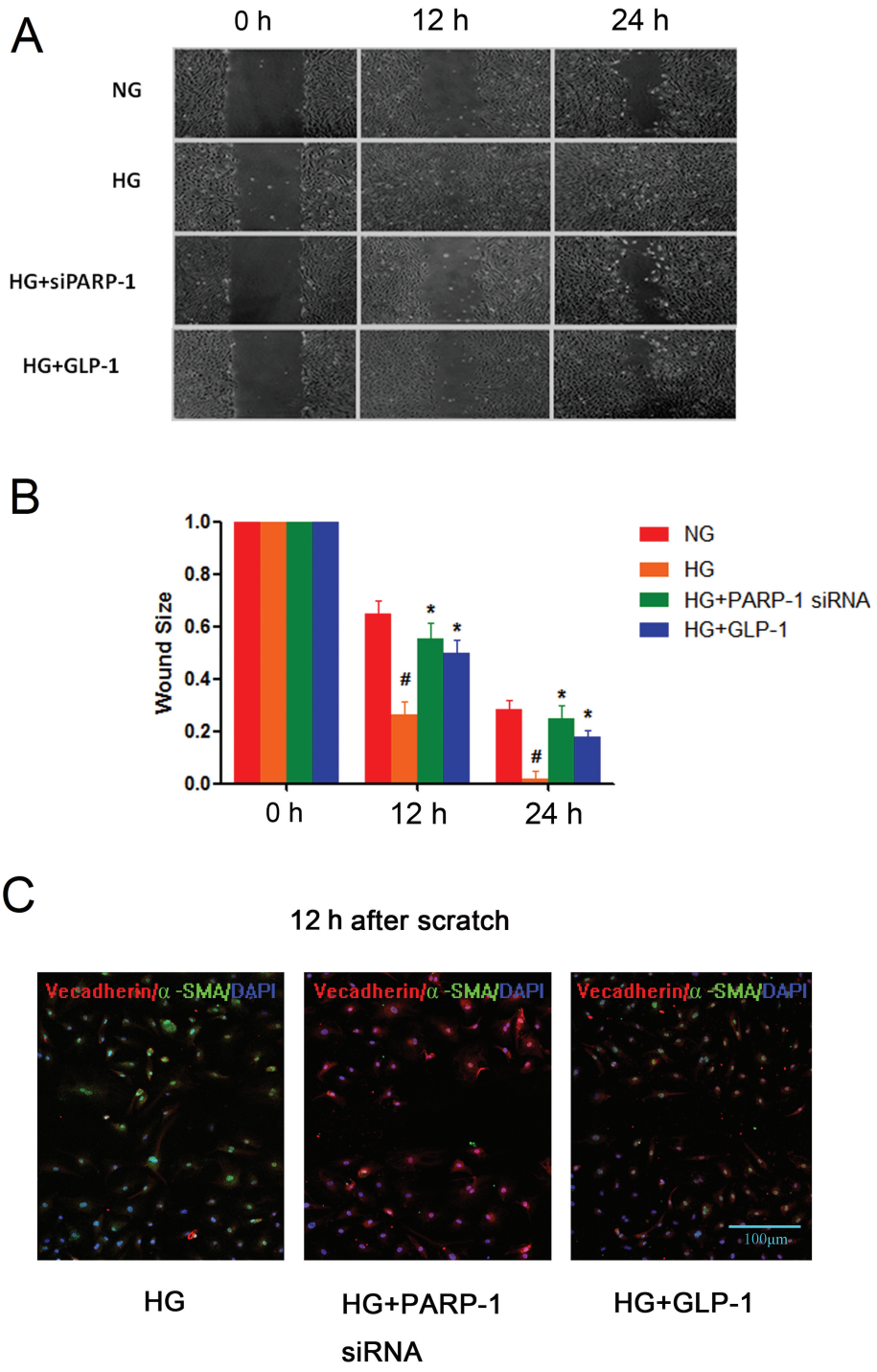

Figure 8. GLP-1 prevented HG-induced endothelial cell migration. (A) Migration immediately after the scratching and 8 and 24 h later. Magnification 10×. Data are from at least three repeated experiments. (B) Quantification of the migration ability at 8 and 24 h after scratching. Data are mean ± SD. $^{\#}p < 0.05$ versus NG, $^{*}p < 0.05$ versus HG. (C) Transitioned endothelial cells (VE-cadherin to α-SMA cell ratio) contribute to faster migration capacity in endothelial cells exposed to HG with siPARP-1 or GLP-1. Double immunofluorescence staining with antibody to VE-cadherin (red) and α-SMA (green). Nuclei were stained with DAPI (blue). Results are from 3 repeated experiments. Scale bar (C), 100 μm.

CONCLUSION

GLP-1 analogs can protect against hyperglycemia-induced EndMT and myocardial dysfunction. This effect may be mediated, at least partially, by suppressing PARP-1 activation. These findings offer an insight into the pathogenesis of diabetic organ fibrosis and may potentially provide a new therapeutic approach to prevent or retard diabetic cardiac fibrosis.

ACKNOWLEDGMENTS

This work was supported by the National 973 Basic Research program of China (no. 2015CB553604), the National Natural Science Foundation of China (81170275, 81370412, and 91439201) and the State Program of National Natural Science Foundation of China for Innovative Research Group (81321061).

DISCLOSURE

The authors declare that they have no competing interests as defined by *Molecular Medicine*, or other interests that might be perceived to influence the results and discussion reported in this paper.

REFERENCES

1. Rosenbloom J, Castro SV, Jimenez SA. (2010) Narrative review: fibrotic diseases: cellular and molecular mechanisms and novel therapies. *Ann. Intern. Med.* 152:159–66.
2. Wei J, Bhattacharyya S, Tourtellotte WG, Varga J. (2011) Fibrosis in systemic sclerosis: emerging concepts and implications for targeted therapy. *Autoimmunity Reviews.* 10:267–75.
3. Wynn TA. (2008) Cellular and molecular mechanisms of fibrosis. *J. Pathol.* 214:199–210.
4. Zeisberg EM, Potenta S, Xie L, Zeisberg M, Kalluri R. (2007) Discovery of endothelial to mesenchymal transition as a source for carcinoma-associated fibroblasts. *Cancer Res.* 67:10123–8.
5. Zeisberg EM, Potenta SE, Sugimoto H, Zeisberg M, Kalluri R. (2008) Fibroblasts in kidney fibrosis emerge via endothelial-to-mesenchymal transition. *J. Am. Soc. Nephrol.* 19:2282–7.
6. Zeisberg EM, *et al.* (2007) Endothelial-to-mesenchymal transition contributes to cardiac fibrosis. *Nat. Med.* 13:952–61.
7. Widyantoro B, *et al.* (2010) Endothelial cell-derived endothelin-1 promotes cardiac fibrosis in diabetic hearts through stimulation of endothelial-to-mesenchymal transition. *Circulation.* 121:2407–18.
8. Li J, *et al.* (2010) Blockade of endothelial-mesenchymal

transition by a Smad3 inhibitor delays the early development of streptozotocin-induced diabetic nephropathy. *Diabetes.* 59:2612–24.
9. Tang RN, *et al.* (2013) Effects of angiotensin II receptor blocker on myocardial endothelial-to-mesenchymal transition in diabetic rats. *Int. J. Cardiol.* 162:92–9.
10. Schraufstatter IU, *et al.* (1986) Hydrogen peroxide-induced injury of cells and its prevention by inhibitors of poly(ADP-ribose) polymerase. *Proc. Nalt. Acad. Sci. U. S. A.* 83:4908–12.
11. Nguewa PA, Fuertes MA, Alonso C, Perez JM. (2003) Pharmacological modulation of poly(ADP-ribose) polymerase-mediated cell death: exploitation in cancer chemotherapy. *Mol. Pharmacol.* 64:1007–14.
12. Szabo C, Zingarelli B, O'Connor M, Salzman AL. (1996) DNA strand breakage, activation of poly (ADP-ribose) synthetase, and cellular energy depletion are involved in the cytotoxicity of macrophages and smooth muscle cells exposed to peroxynitrite. *Proc. Nalt. Acad. Sci. U. S. A.* 93:1753–8.
13. Du X, *et al.* (2003) Inhibition of GAPDH activity by poly(ADP-ribose) polymerase activates three major pathways of hyperglycemic damage in endothelial cells. *J. Clin. Invest.* 112:1049–57.
14. Chiu J, Xu BY, Chen S, Feng B, Chakrabarti S. (2008) Oxidative stress-induced, poly(ADP-ribose) polymerase-dependent upregulation of ET-1 expression in chronic diabetic complications. *Can. J. Physiol. Pharmacol.* 86:365–72.
15. Chiarugi A, Moskowitz MA. (2003) Poly(ADP-ribose) polymerase-1 activity promotes NF-kappaB-driven transcription and microglial activation: implication for neurodegenerative disorders. *J. Neurochem.* 85:306–17.
16. Mota RA, *et al.* (2008) Poly(ADP-ribose) polymerase-1 inhibition increases expression of heat shock proteins and attenuates heat stroke-induced liver injury. *Crit. Care Med.* 36:526–34.
17. Rieder F, *et al.* (2011) Inflammation-induced endothelial-to-mesenchymal transition: a novel mechanism of intestinal fibrosis. *Am. J. Path.* 179:2660–73.
18. Monji A, *et al.* (2013) Glucagon-like peptide-1 receptor activation reverses cardiac remodeling via normalizing cardiac steatosis and oxidative stress in type 2 diabetes. *Am. J. Physiol. Heart Circ. Physiol.* 305:H295–304.
19. Noyan-Ashraf MH, *et al.* (2013) A glucagon-like peptide-1 analog reverses the molecular pathology and cardiac dysfunction of a mouse model of obesity. *Circulation.* 127:74–85.
20. Poornima IG, Parikh P, Shannon RP. (2006) Diabetic cardiomyopathy: the search for a unifying hypothesis. *Circ. Res.* 98:596–605.
21. Battiprolu PK, Gillette TG, Wang ZV, Lavandero S, Hill JA. (2010) Diabetic cardiomyopathy: mechanisms and therapeutic targets. *Drug Discov. Today.* 7:e135–43.
22. Liu FQ, *et al.* (2011) Glucagon-like peptide 1 protects microvascular endothelial cells by inactivating the PARP-1/iNOS/NO pathway. *Mol. Cell. Endocrinol.* 339:25–33.
23. Shevalye H, Maksimchyk Y, Watcho P, Obrosova IG. (2010) Poly(ADP-ribose) polymerase-1 (PARP-1) gene deficiency alleviates diabetic kidney disease. *Biochim. Biophys. Acta.* 1802:1020–7.
24. Committee for the Update of the Guide for the Care and Use of Laboratory Animals, Institute for Laboratory Animal Research, Division on Earth and Life Studies, National Research Council of the National Academies. (2011) *Guide for the Care and Use of Laboratory Animals*. 8th edition. Washington (DC): National Academies Press.
25. Hou A, *et al.* (2013) Rho GTPases and regulation of cell migration and polarization in human corneal epithelial cells. *PLoS One.* 8:e77107.
26. Medici D, Potenta S, Kalluri R. (2011) Transforming growth factor-beta2 promotes Snail-mediated endothelial-mesenchymal transition through convergence of Smad-dependent and Smad-independent signalling. *Biochem. J.* 437:515–20.
27. Gao H, Zhang J, Liu T, Shi W. (2011) Rapamycin prevents endothelial cell migration by inhibiting the endothelial-to-mesenchymal transition and matrix metalloproteinase-2 and -9: an in vitro study. *Mol. Vis.* 17:3406–14.
28. Lee CH, *et al.* (2011) Ischemia-induced changes in glucagon-like peptide-1 receptor and neuroprotective effect of its agonist, exendin-4, in experimental transient cerebral ischemia. *J. Neurosci. Res.* 89:1103–13.
29. Matsubara J, *et al.* (2012) A dipeptidyl peptidase-4 inhibitor, des-fluoro-sitagliptin, improves endothelial function and reduces atherosclerotic lesion formation in apolipoprotein E-deficient mice. *J. Am. College Cardiol.* 59:265–76.
30. Ban K, *et al.* (2008) Cardioprotective and vasodilatory actions of glucagon-like peptide 1 receptor are mediated through both glucagon-like peptide 1 receptor-dependent and -independent pathways. *Circulation.* 117:2340–50.
31. Bullock BP, Heller RS, Habener JF. (1996) Tissue distribution of messenger ribonucleic acid encoding the rat glucagon-like peptide-1 receptor. *Endocrinology.* 137:2968–78.
32. Goumans MJ, van Zonneveld AJ, ten Dijke P. (2008) Transforming growth factor beta-induced endothelial-to-mesenchymal transition: a switch to cardiac fibrosis? *Trends Cardiovasc. Med.* 18:293–8.
33. Kumarswamy R, *et al.* (2012) Transforming growth factor-beta-induced endothelial-to-mesenchymal transition is partly mediated by microRNA-21. *Arterioscler. Thromb. Vasc. Biol.* 32:361–9.
34. Choi SK, *et al.* (2012) Poly(ADP-ribose) polymerase 1 inhibition improves coronary arteriole function in type 2 diabetes mellitus. *Hypertension.* 59:1060–8.
35. Li WJ, Shin MK, Oh SJ. (2011) Poly(ADP-ribose) polymerase is involved in the development of diabetic cystopathy via regulation of nuclear factor kappa B. *Urology.* 77:1265.e1–8.
36. Rodriguez MI, *et al.* (2011) Poly(ADP-ribose)-dependent regulation of Snail1 protein stability. *Oncogene.* 30:4365–72.
37. Shiraki A, *et al.* (2012) The glucagon-like peptide 1 analog liraglutide reduces TNF-alpha-induced oxidative stress and inflammation in endothelial cells. *Atherosclerosis.* 221:375–82.
38. Wang D, *et al.* (2013) Glucagon-like peptide-1 protects against cardiac microvascular injury in diabetes via a cAMP/PKA/Rho-dependent mechanism. *Diabetes.* 62:1697–708.
39. Hendarto H, *et al.* (2012) GLP-1 analog liraglutide protects against oxidative stress and albuminuria in streptozotocin-induced diabetic rats via protein kinase A-mediated inhibition of renal NAD(P)H oxidases. *Metab. Clin. Exp.* 61:1422–34.

Cite this article as: Yan F, *et al.* (2015) Glucagon-like peptide 1 protects against hyperglycemic-induced endothelial-to-mesenchymal transition and improves myocardial dysfunction by suppressing poly(ADP-ribose) polymerase 1 activity. *Mol. Med.* 21:xx–xx.